EFFECT OF LaF_3 ON THERMAL PROPERTIES, CRYSTALLIZATION AND SINTERING OF SEALING GLASS-CERAMIC

[#]A. FAEGHINIA

Ceramic Division, Materials and Energy Research Center (MERC), P. O. Box: 14155-4777, Tehran, Iran

[#]E-mail: aida.faeghinia@gmail.com

Submitted November 09, 2013; accepted March 7, 2014

Keywords: Seal glass, TEC, Sintering, Crystallization

In this work one type of seal glass containing 0, 2 and 4 wt. % LaF_3, were prepared. Crystallization and the sintering behavior of obtained glasses were compared. By adding LaF_3 the bulk crystallization via lithium disilicate was promoted. The aspect ratio of resulted microstructure was increased by LaF_3 amount. Also the TEC and the wetting angle of LaF_3 bearing glasses raised up to 36 % and 122° respectively.

INTRODUCTION

Several commercial glass-ceramics are used for seals to metals. lithium aluminum silicate glass–ceramics are perhaps best known for very low expansion materials based on beta spodumene or beta eucryptite. Other compositions in that system are capable of being crystallized to much higher TEC (Thermal expansion coefficient) values [1]. The crystallization properties of this lithium silicate system were investigated by small addition of K_2O, Al_2O_3, B_2O_3, P_2O_5 using a standard heat treatment procedure [2]. Normally P_2O_5 acts as a nucleating agent and the major crystalline phases that can be formed in this system are lithium metasilicate and lithium disilicate, together with various silica phases, e.g. cristobalite, quartz or tridymite. Depending on the presented phases, glass-ceramics can be produced, with TEC in the range of 8 - 19 × 10^{-6} (°C) [3]. Within this system, the seal of a La-doped glass, was found to be fairly good with Ti based alloys, and the bulk glass characterization was studied [4]. But the effect of LaF_3 bearing seal glass in binding with the Fe based alloys was not studied. Furthermore in the case of Fe based alloys it was shown that by using the transition metal oxide additive in starting glass sealant the undesirable effect of water reaction was minimized [5]. Also, La_2O_3 as a modifier in the glass composition controls the viscosity of the glass sealant at SOFC operational condition [6] but the sintering behavior of these La bearing systems was not studied. On the other hand, it is well known that the thermal stresses in sealing system are commonly observed due to mismatch of thermal expansion coefficient (TEC) between glasses and alloys [7], conversely crystallization in glass seals is reported to show better physical properties but it causes serious TEC mismatch [8], which affects the seal performance. Thus, crystallization of glass sealants is an important factor related to thermal stress distribution and mechanical integration in seal stack. The glass sealant should have controlled crystallization and the crystalline phases should be stable so that the sealant can be used for long time [9]. For very high strength requirements, glass-ceramic/metal seals that utilize precipitation-hardenable superalloys, such as Inconel 718, have been developed. However, these superalloys have various deficiencies which have limited their usefulness in various applications [7]. From experience, it has been determined that these superalloys are tricky to machine and are very temperamental in their welding characteristics. When high strength is not a requirement, other materials such as stainless steels may be preferred. A stainless steel, such as 304L, is a widely available material which is easy to machine and has very good weldability, particularly when compared to a superalloy. Because of these advantages, research was undertaken to fabricate glass-ceramic/metal seals utilizing 304L.

We have selected a group of Li_2O–LaF_3–Al_2O_3–B_2O_3–SiO_2 –P_2O_5-ZnO based glasses (according to [4]) with 2 and 4 wt. % LaF_3. The objective of this work was the investigation on the thermal properties to evaluate LaF_3 bearing glass suitability as sealant materials for 304L. Crystallization and sintering of these compositions changes in the TEC and crystallization process have been evaluated.

EXPERIMENTAL

Glasses preparation

The mixtures of reagent grade chemicals, K_2CO_3, ZnO, Al_2O_3, Li_2CO_3, B_2O_3, P_2O_5, LaF_3 and pure optical grade silica, were melted in platinum crucible at temperatures ranging from 1380°C to 1400°C in an electric furnace for –2 h a lid was used in order to avoid flour loss. The glass composition was selected according to [4] and the LaF_3 was added in 2 and 4 wt. % at the composition of the base glass.

The resulting melts were quenched in cold distilled water. In all glasses frits no crystalline phases were detected by XRD. The nominal chemical composition of glasses is displayed in Table 1.

Table 1. The chemical composition of studied glass in wt. % the $LaF_3$was added in excess.

Wt. %	Base	La2	La4
Li_2O	12.6	12.6	12.6
ZnO	1.8	1.8	1.8
AL_2O_3	3.9	3.9	3.9
SiO_2	74	74	74
B_2O_3	4.7	4.7	4.7

Thermal characterization

The frits were ground in an agate mortar, and sieved to give fine (< 45 μm) for subsequent use in pressed samples.

DTA differential thermal analysis, Netzsch320, which was utilized to determine the crystallization temperature of glasses, was performed by using 6 mg of glass powders in an alumina crucible in air with a heating rate of 10°C/min. Alumina was used as an inert reference material.

The thermal expansion coefficient measurements were carried out in a dilatometer (model- Netzsch: -E402). The glass-ceramics were in sintered form and the glasses were in bulk form.

The heating rate was kept to 10°C/min for all measurements. The size of the samples was kept at a max. of 20 mm height and 5 mm diameter with both ends flat. The samples were kept in a quartz sample holder with a constant load of 5 g for all measurement. The expansion coefficient being reported is the average in the temperature range of 30 - 800°C. The reference material used for correction of holder expansion was Alumina.

Sample preparation

The fine glass powders (< 45 μm) were mixed with 2.5 wt. % polyvinyl alcohol as a binder and pressed into 10 mm diameter and 10 mm high disks at a pressure of 10 MPa using a laboratory uniaxial hydraulic press. Besides for preparing the bulk sample, the melts were poured into a graphite mould of max. 75 mm diameter and 30 mm height. This was immediately transferred to annealing furnace and maintained at around 450°C for 1 - 2 h. After annealing the glass was cooled to room temperature at the rate of 20°C/h. In order to transform the glass to a glass ceramic, controlled crystallization was carried out in a programmable vertical tubular furnace. The heat treatments were performed at the temperature corresponding to the DTA peaks with a heating rate of 10°C /min in an electric furnace.

The densities of the glasses and the corresponding glass-ceramics were measured by AccuPyc1330 pycnometer, which measures the volume of solid objects with regular or irregular shapes as well as of powder samples. The pycnometer determines volume by measuring the change of the pressure of helium in a calibrated volume. The experimental error in the measurements, employing a bulk glass or glass-ceramic sample of about 3 - 4 g, was evaluated as ± 0.001g cm^{-3}.

Three samples dimensions were measured before and after heat treating to obtain shrinkage data and the standard deviation (error bars) was reported.
The porosities were measured using water absorption method.

Phase evaluation

Crystallization products (glass-ceramics) in powder form were identified by XRD (Philips power diffractometer 1710). CuKα radiation was used in XRD examinations. Working voltage and current were 40 kV and 80 mA, respectively, also the step size plus step time were 0.04° and 0.75 s respectively.

Oxidation of the 304L steel

Sample of 304L steel with chemical analysis of presented data in Table 2 was chosen. (The presented chemical composition is in wt. % form which was measured by XRF). The samples were obtained by cutting annealed 1.5 in. diameter. 304L bar stock in to disks of 2 mm thickness, which were then cut into quarter-disk coupons for testing. The samples were cleaned with alcohol and dried prior to oxidation. Pre-oxidation of samples was performed according to [10]. The Pre-oxidation of samples was performed at 1000°C for 90 minutes in a low p_{O2} atmosphere and 0.02 g/cm^2 weight was gained.

Table 2. Chemical composition of studied 304L alloy in wt. %.

O_2 (wt. %)	Zn (wt. %)	Si (wt. %)	Mg (wt. %)	Cr (wt. %)	Fe (wt. %)
7.3	0.1	0.8	0.1	25.1	67.2

After cool down from the pre-oxidation treatment, glass sealing properties were performed on samples. A small piece of pressed glasses were placed on the pre-oxidized 304L steel surface, and then the systems were heated at the given temperatures (according to Figure 1) in oxygen atmosphere. The samples were holed long enough for glass flow and drop formation, and then cooled to room temperature. During this experiment the glass softens and forms a hemispherical cap on the pre-oxidized metal surface. The experiments are used as a qualitative measure of the glass adhesion. The two dimension image of glass wetting angle on the steel was measured using Conveyor. The specialized time-temperature sealing/crystallization cycle was according to the cycle shown in Figure 1. The cycle was not difficult to perform and could be accomplished in any reasonable programmable furnace typically used in forming glass-ceramic compositions.

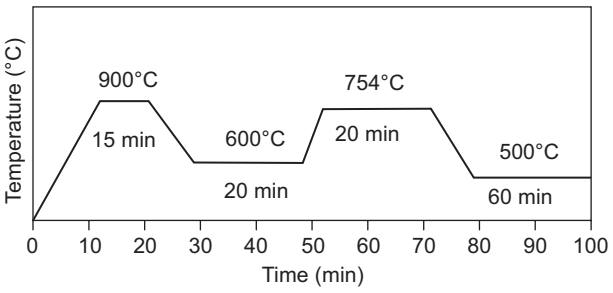

Figure 1. The heat treatment program of pressed frites (La4, La2, B) in disc form.

The samples microstructure in scanning electron microscopy (SEM - TESLA BS 300) with digital unit (TESCAN) was evaluated. The electron probe micro-analyzer analysis (EPMA JEOL JXA-840A, EDS parameters – 15 KV, Takeoff Angle 40.0°) was used to analyze the samples crystals.

RESULTS AND DISCUSSION

Figure 2 depicts the glasses DTA curves and the characteristic temperatures of glasses were presented in Table 3. First and the last inflexion point of DTA traces were taken to the T_g (glass transition) and T_d (softening temperature) of glasses respectively.

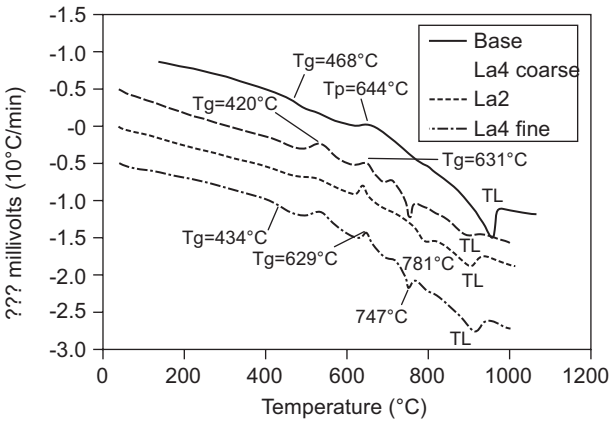

Figure 2. DTA curves of obtained B, La2, La4 glasses with 45 micron size, (the coarse one indicated to the 2 mm frit size of La4).

As seen in the La4 and La2 DTA curves, the crystallization peaks (T_p) at around 630°C became sharper, associated to the bulk crystallization trend. Moreover the T_g, T_d and T_L (liquidus temperature) of the LaF_3 bearing systems were diminished.

A lower T_d with the addition of LaF_3 is due to the effect of fluorine ions (network modifier) in the glass structure, which creates non-bridging oxygen and thus the glass network is less rigid and the viscosity also decreases [12].

Furthermore no difference in the DTA curves of the fine and coarse La4 frits was observed (Table 3 and Figure 2), again designated to the bulk nucleation mechanism in this system.

On the basis of characteristic temperatures, the Saad-Poulian factor, H [13], was defined. This factor was as: Equation (1)

$$H = T_p - T_g/T_g \quad (1)$$

where T_p is the beginning temperature of crystallization and T_g is the glass transition temperature). H was determined to evaluate the glass-forming ability of the studied glasses. It is common knowledge that, the higher the H values, the higher the thermal stability of material and the lower its susceptibility to crystallization. The H values were measured according to Equation 1 and the results were presented in Table 3. And it is obvious that, by using LaF_3 (in 2 - 4 wt. %), the H factor was decreased

Table 3. Characteristic temperatures (°C) and densities of studied glasses with fine (45 μm) and coarse (1 mm) grain size ,T_g - glass transition temperature, T_d - softening temperature, T_p - crystallization temperature, T_L - liquidus temperature.

Sample	T_g (°C)	T_d (°C)	T_{P1} (°C)	T_{p2} (°C)	T_{p3} (°C)	T_L (°C)	H	Density (g cm^{-3})
B (fine)	468	521	644	–	–	944	0.27	2.32
La2 (fine)	434	497	528	631	746	885	0.14	2.46
La4 (fine)	420	447	513	629	750	895	0.10	2.54
La4 (coarse)	419	440	511	635	749	886	0.10	2.54

Sintering behavior

Since most of the seal rings were prepared by the sintering process, the pressed samples were isothermally sintered at 780, 820, 860°C for 1 h respectively.

Figure 3, Figure 4 and Figure 5 depict the porosity, the axial and radial shrinkage (%) of the glasses with the sintering time..

In Figure 3, the porosity was reduced from 30 % to 13 % at 780°C by the sintering time in base glass and almost to 6 % in the LaF_3 bearing system. To justify this different trend in three samples prosities, the viscosity variations, were estimated by the Lakatos method in the investigated 780 - 860°C temperature range [16]. In this manner the shear viscosity of the LaF_3 bearing system was calculated 10^5 dPa while this value was calculated almost $10^{5.5}$ dPa for the base glass at 780°C, according to Frenkel theory in Equation (2):

$$t = 4\,\eta a_0/3\delta \qquad (2)$$

where δ is the surface tension, η is the viscosity, a_0 is the radius of the particles, t is sintering time.

As the viscosity of the base glass was calculated higher than the others, the sintering time of the base glass was expected to be about 2 times longer than the LaF_3 bearing systems at the 780°C so instead of increasing the sintering time inevitably the sintering temperature was increased to 820°C.

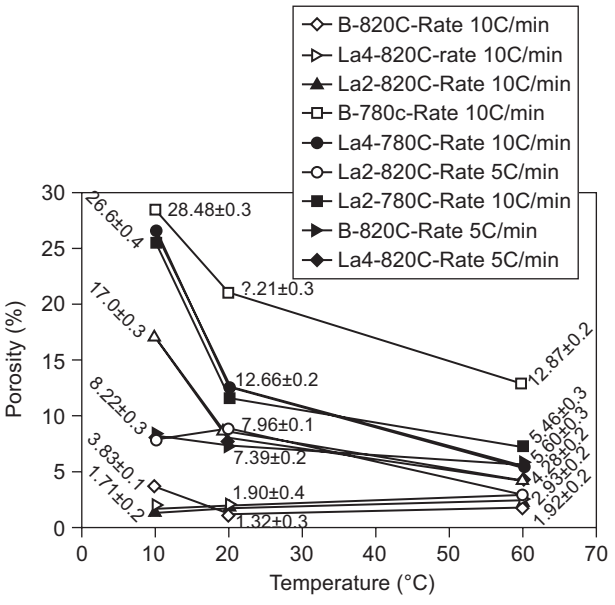

Figure 3. The porosity of pressed sintered B, La2, La4, vs. sintering time at 780°C, 820°C with 10°C/min and 5°C/min heating rate.

The high densification rate of the La2 and La4 at 820°C can be seen and explained by the flux effect of the fluoride ion in the remaining glass, led to the high densification rate. [14, 15].

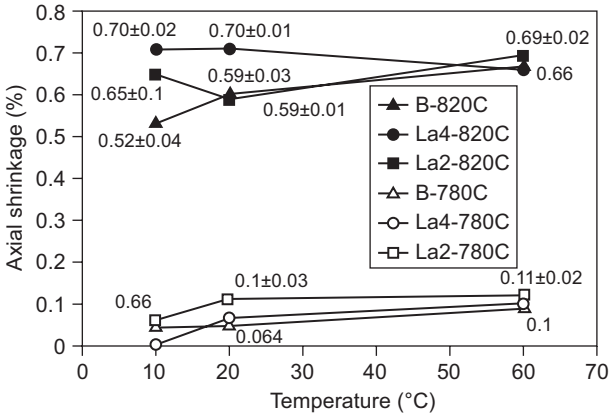

Figure 4. The axial shrinkage % of B, La2, La4 vs. sintering time at 780°C, 820°C with 10°C/min heating rate.

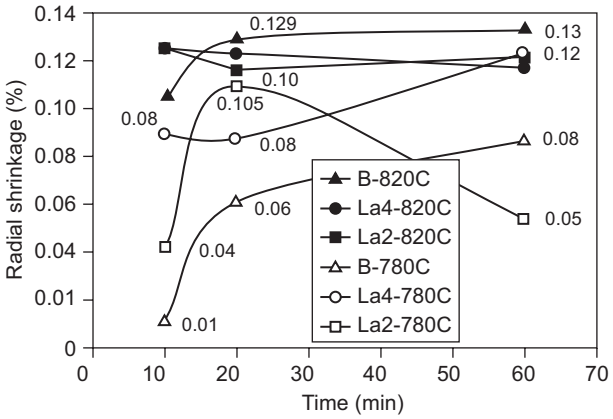

Figure 5. The radial shrinkage % of sintered La2, La4, B vs. time at 780°C, 820°C with 10°C/min and 5°C/min heating rate.

Also in the sintered samples, while the sintering behavior was degraded by the heating rate (5°C/min), the noticeable density's difference was not seen among 10 and 20°C/min heating rate. Furthermore at the 860°C, the base glass was deformed and the La2 and La4 were densified.

By comparing the resulted radial and axial shrinkages with the sintering time and temperature (Figures 4 and 5), although no significant changes in the La2 and La4 radial dimensions were observed, the axial shrinkage, were altered with the time and temperature. This anisotropy in shrinkage can be described by the geometrical rearrangement of the particles during uniaxial pressing [17].

X-ray diffraction and crystallization results

On the basis of the DTA results, glasses were heat treated at the first, second DTA exo-peak and the sintering temperatures. The phase's evaluation was depicted in Figure 6.

Figures 6b and 6c, depict that, lithium metasilicate, besides the lanthanum silicate, was developed as the major crystalline phase at the first peak (630°C) in La2 and La4. The crystallization of lanthanum silicate phase in other silicate glass was observed as well. It was reported that in $10K_2O{\cdot}50SiO_2{-}nLa_2O_3$ systems [18], lanthanum coordinates with silicate anions in glasses; the solution chemistry of lanthanum in these glasses, is governed by homogeneous equilibria between different silicates anions bonded to lanthanum. On the other hand it was pointed implicitly [19] that, reaction of silicon and rare oxide in the excess oxygen atmosphere is thermodynamically preferred, these facts may explain the lanthanum silicate formation in our glass-ceramics systems. Moreover the lanthanum silicate formation can be explained by the well known strong tendency of La^{3+} ion to act as very efficient nucleating agents in glasses due to their high field strength. Entirely the LaF_3 containing glasses, have contributed in the formation of $La_4Si_3O_{12}$ which probably promoted the growth of lithium metasilicate phase.

Headly [20] has reported the epitaxial growth of lithium metasilicate on lithium phosphate in LAS (lithium–aluminum–silicate) glass-ceramics, but the effect of lanthanum silicate on crystal growth of lithium metasilicate was not clear. Besides the lithium disilicates, as the major phase in all samples, quartz and lithium aluminum silicate, were detected in LaF_3 bearing and the base glass, at the 820°C, respectively (Figure 6a).

It is well known that [21], in some lithium silicate glasses lithium metasilicate crystallization, precedes the lithium disilicate crystallization as a metastable phase and crystallizes at a lower temperature. On the other hand it was shown that [21], as the Li_2O content increases over the stoichiometric content of lithium disilicate, lithium metasilicate crystallized and other crystalline phases can be formed depending on the starting glass composition. In the present work by using LaF_3, probably the remaining glass composition was modified; leading to the quartz crystallization beside the disilicate phase.

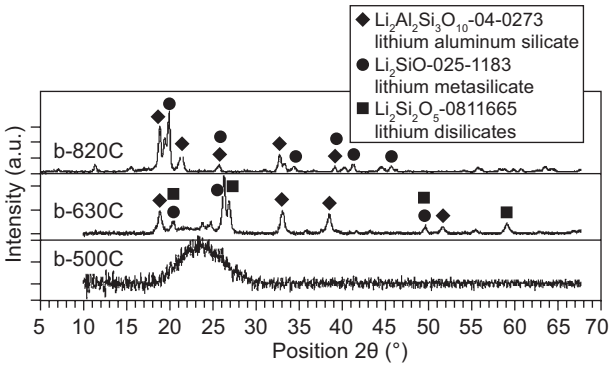

a) base sample

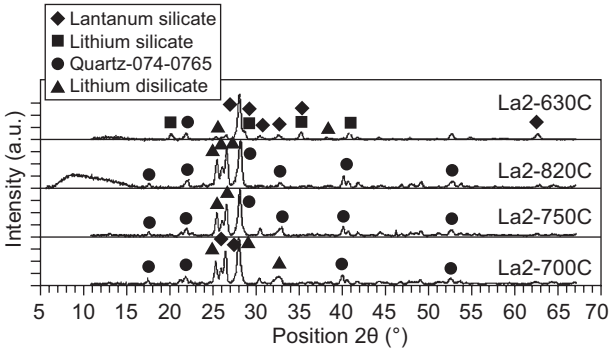

b) La2

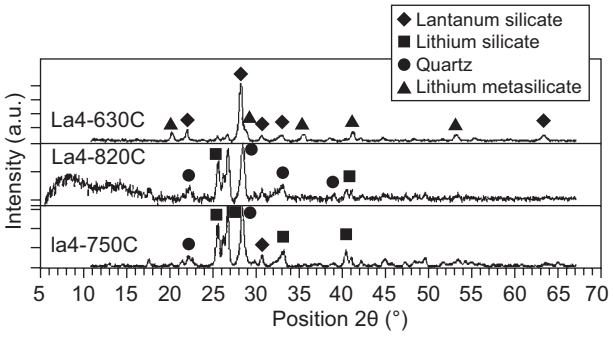

c) La4

Figure 6. The XRD results of heat treated samples at 630°C, 700°C, 750°C, 820°C: a) base sample, b) La2, c) La4.

Microstructural evaluation of prepared glass

The heat treated bulk base and La2 glasses were crystallized, at 860°C. Figures 7a, b, c show the SEM micrographs of La2 microstructure with the different crystals morphology, and the approximate chemical compositions were measured by the EPMA (electron probe micro analyzer) and were reported in Table 4.

Table 4. The EPMA analysis of the pointed images the chemical analysis of pointes are presented in wt. %.

wt. %	Al_2O_3	SiO_2	P_2O_5	K_2O	Zno	ZrO_2
1	1.5	81.1	6.9	5.7	4.8	0.0
2	4.0	87.7	1.9	0.8	5.5	0.0
3	3.4	84.5	5.7	3.3	2.7	0.4
4	3.7	85.3	4.3	3.0	3.1	0.4

In the La2 glass-ceramic (Figure 7b) the lath-shaped crystals which were close to the irregular shape of hexahedral, demonstrated 25 micron in length and 5 micron in width. These crystals by considering the chemical composition of point 2 can be related to the lithium disilicate [22, 23]. Also the crystals with similar composition (point 4) were detected in the base glass-

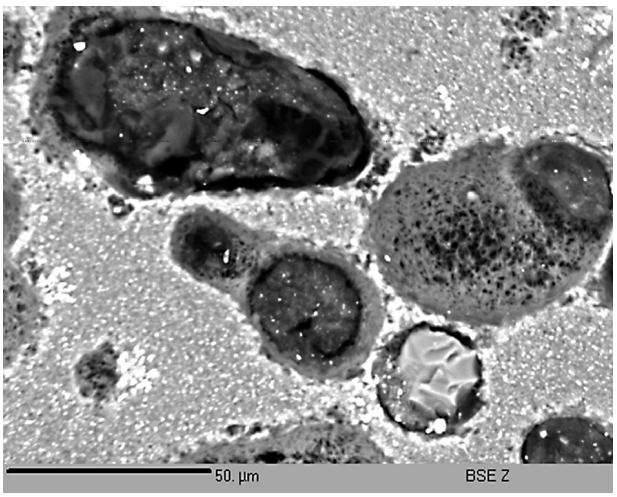

a) La2 860°C

ceramic, apparently pointed to the lithium disilicate crystals. Conversely in the La2 glass-ceramic, the mentioned crystals had relatively higher aspect ratio than the faceted crystals in the base glass-ceramic (Figures 7d,e)

On the other hand, regarding to the chemical composition of point 1, the dendritic crystals; with no specific growth direction, can be related to the lithium metasilicate [24] the crystals morphology within two (La2 and base) systems was not different (Figure 7c). Moreover some detected light regions, assumed to the existed heavy elements, like lanthanum in La2.

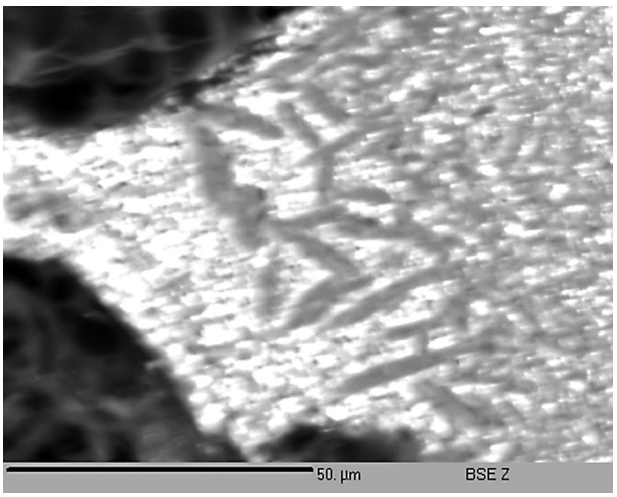

b) La2 860°C

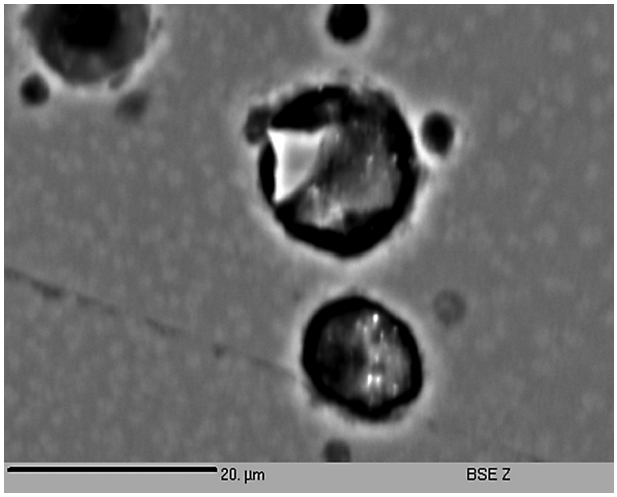

d) La2 860°C

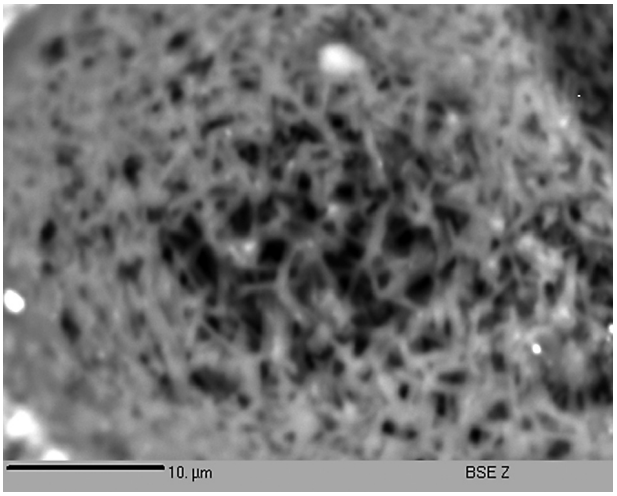

c) b glass-ceramic 860°C

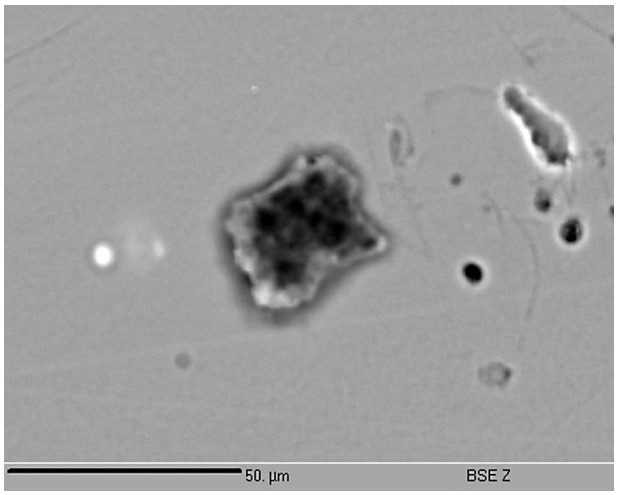

e) lithium disilicate

Figure 7. SEM micrographs of: a) La2 glass-ceramic heat treated at 860°C with lath shape lithium disilicate crystals; b) La2 at 860°C with denderitical crystal form of lithium meta silicate; c) b glass-ceramic heat treated at 860°C; e) lithium disilicate in base glass-ceramic detected at 860°C.

Thermal properties of glasses

Figure 8 shows the bulk glasses and 304L alloy dilatometric curves. The obtained results of the dilatometries in glasses and 304 L alloy were summarized in Table 5.

The base glass TEC varies between 7.34 - 8.11 × 10^{-6} °C but the La2 and La4 showed high TEC values, deduced to the decreased glass network connectivity, however the TEC values of both glasses were lower than those of 304 L. Conversely lower T_g (468°C) than sealing temperature (860°C) is favorable in these systems. It is well known that, the stress due to thermal expansion mismatch always develop below sealing temperature, whereas the stress arising from TEC mismatch above T_g can be tolerated by the glass sealant, due to its viscous flow at sealing temperature. The thermal stress δ which arises due to TEC mismatch between the glass and metals, is given by the following relation [7]: Eq.3

$$\delta = CE \int (\alpha_g - \alpha_m)\, dT \quad (3)$$

where E is Young`s modulus , C is geometrical constant, and α_g, α_m are TEC of glass and metal. The TEC of glasses and 304L alloy has been shown in Figure 8. It is observed that the maximum TEC mismatch occurs at near T_g, so in order to increasing the TEC of glass samples, the bulk form of glasses, were heat treated at the sealing temperature and the resulted glass-ceramics were analyzed by dilatometry.

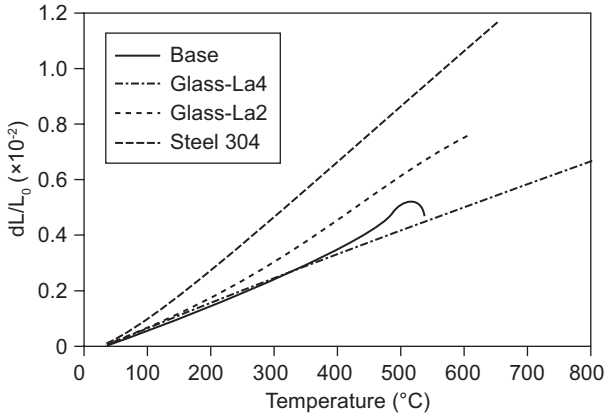

Figure 8. The dilatometer results of B, La2, La4 glasses and 304L alloy.

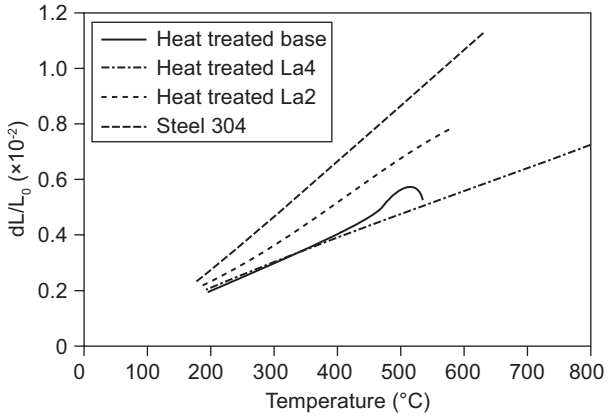

Figure 9. The dilatometer results of base glass and the heat treated glasses at 820°C.

Thermal properties of glass-ceramics

The TEC of obtained sintered glass-ceramics are shown in Figure 9. The heat treated La2 at 820°C, exhibited α = 13.24 × 10^{-6} (°C) from room temperature to 600°C but the base glass, crystallized at 820°C exhibited α = 11.20 × 10^{-6} °C. It was mentioned before in Figure 6 that the lithium disilicate and lithium aluminum silicate were the existed crystalline phase in base glass-ceramic, it is thought that, although the lithium disilicate phase exhibits high thermal expansion (like 30×10^{-7} °C) from room temperature to 600°C [23, 24], but the low thermal expansion of the lithium aluminum silicate phase, counteracted the high thermal expansion of lithium disilicate phase in base glass-ceramic. The high value of La2 TEC, correlated to the SiO_2 crystallization content, appeared at 820°C. It was reported before [17] the SiO_2 crystallization in silicate glass, can modify the glass network, reduces the structural rigidity, and increases the density (Table 3) and the TEC (Figure 8). Moreover

Table 5. TEC of obtained samples at different temperatures ranges.

	Glass B	Glass La2	Sample 304	Glass La4	Glass-ceramic La2	Heat treated B	Heat treated La4 (2 steps heating)	Heat treated La2 (2 steps heating)
α: RT 100°C	6.8	7.2	13.4	7.6	8.8	7.9	7.9	8.4
α: RT 150°C	7.5	7.7	14.9	8.1	–	–	–	9.9
α: RT 200°C	7.8	8.0	15.9	8.4	11.1	8.9	9.2	11.9
α: RT 250°C	8.2	8.4	16.6	8.7	–	–	–	12.6
α: RT 300°C	8.6	8.7	17.2	8.9	12.1	9.8	9.9	13.2
α: RT 350°C	8.9	9.0	17.6	9.2	–	–	–	13.6
α: RT 400°C	9.2	9.3	17.9	9.7	13.4	10.4	11.2	14.9

Note: all values: ×10^{-6}.

there are correlations between the high density along with TEC, in La2 and base glass-ceramics but the TEC mismatch has not solved yet, so the pressed samples were crystallized in 2 steps heat treating (according to Figure 1) and the TEC of resulted glass-ceramics were measured by the dilatometry, the results were presented in Table 5 as well. Obviously by increasing the heat treatment steps, the TEC of glass-ceramics was increased, the variation of the glass ceramic TEC may be explained on the basis of different crystalline phases and quantity of each phase at various stages of sintering. As discussed previously, two crystalline phases evolved out of the glass on heat treatment, i) quartz, ii) lithium disilicate. In this case of glass devitrification, in the initial steps of heat treatment the lanthanum silicate phase was evolved in the glass matrix which led to a decrease in the TEC of the glass ceramics. On the two steps sintering, the TEC probably was increased with emergence of lithium disilicate phase. However, to establish an exact correlation between volume of various phases present in the glass ceramics and the TEC of the glass ceramics is difficult as with formation of crystalline phases, the composition of the remaining glass matrix changes, thereby its TEC may be changing. In fact it needs to carry out a further detailed analysis between different phases present in the glass ceramics and their contribution towards thermal expansion of the matrix using the standard additive rule [23]. However the two steps heat treatment were performed on seal glass and the produced seal systems were qualified in point view of wetting angle.

Wetting behavior

Figure 10 shows the hemispherical shape of pressed samples adhered on the oxidized 304L which were heat treated according to Figure 1. The wetting angle for La4, La2 and b glass were measured as mentioned above and were obtained 122°, 111.5°, 95 respectively. It is interesting that the wetting angles for the pre-oxidized steel and glass seal conditions were essentially the same for the three glasses. The differences in wetting angle results can be related to the glass composition and it can be concluded that the lanthanum bearing systems has low viscosity and spread more than base glass at sealing temperature on oxidized 304L, but however the adherent quality of these system should be estimated by bending strength measurement [24].

CONCLUSION

Thermal stability of seal glass with LaF_3 additive in LAS system was studied. It was shown that by LaF_3 addition, the bulk crystallization trend was increased through the decreased T_g and H values in the base glass. The sintering temperature of La bearing system was found at 860°C.

The crystallization of La4 and La2 systems were through lanthanum silicate and lithium metasilicate at low (630°C) temperature and prolonged by quartz formation at high (820°C) temperature. The glass TEC was found to be related to the quartz phase amount which formed during crystallization. Furthermore by comparing the increased values of TEC (up to 1×10^{-6} °C) in LaF_3 bearing systems with base glass, it can be concluded that LaF_3 has increased the seal glass`s TEC. Also the 2 step heat treating of La2 glass-ceramics has found 14.9602×10^{-6}/°C thermal expansion.

The effect of the LaF_3 on crystalline morphology of lithium disilicate was investigated by the SEM method. It has been found that the addition of LaF_3 increases the aspect ratio of resulted lithium silicate.

The adherence of La4 to 304l was improved, which can be attributed to decreased glass surface tension of this glass.

REFERENCES

1. McMillan P.W.: Glass Ceramics, p. 245-266, Academic Press, 1979.
2. Borom M.P., Turkalo A.M., Doremus R.H.: J. Am. Cer. Soc. *58,* 385 (1975).
3. Lin C. K., Chen T. T.: J. Power Sources *164,* 238 (2007).
4. Donald I.W.: J. Mat. Sci. *28,* 2841 (1993).
5. Donald I.W., Mallinson P.M.: J. Mat. Sci. *46,* 1975 (2011).

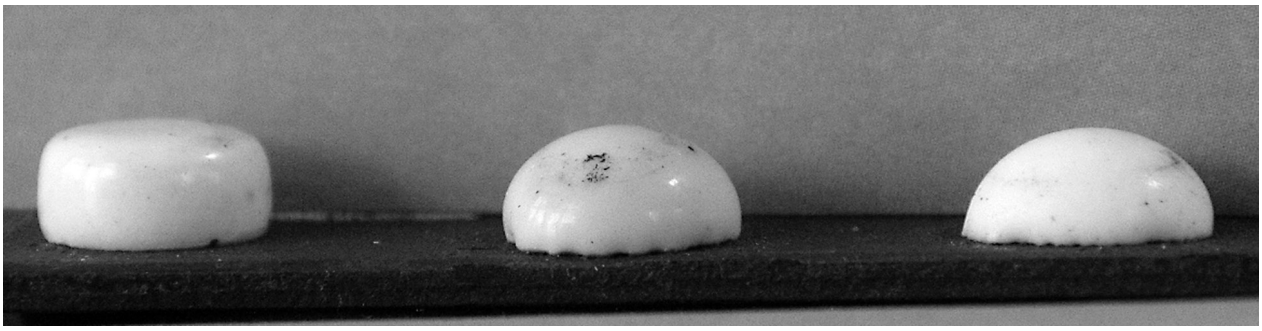

Figure 10. The images of hemispherical shape of deformed B, La2, La4 on 304L, heat treated at 2 steps heat treating.

6. Hao J., Zan Q.: J. Pow. Sour. *214,* 75 (2012).
7. Montross C.S., Yokokawa H., Dokiya M.: Br. Ceram. Trans. *101,* 85 (2002).
8. Atkinson A., Sun B.: Mater. Sci. Technol. *23,* 1135 (2007).
9. Kumar P., Chongdara T.K.: J. Power. Sour. *221*, 28 (2013).
10. Susan D.F.: *Mechanical Properties and Performance of Engineering Ceramics II: Ceramic Engineering and Science Proceedings,* p. 145-157, John Wiley & Sons, Inc., 2008.
11. Kord M., Marghussian V.K., Eftekhari-yekta B., Bahram A.: J. Non. Cryst. Sol.: *355,* 141(2009).
12. Romanowski R.: J. Rare Earths *28*, 893 (2010).
13. Sroda M.: J. Therm. Analys. Cal.: 88, 245 (2007).
14. Salman S.M., Darwish H., Mahdy E.A.: Cer. Int. *34*, 1819 (2008).
15. Lara C., Pascual M.J., Durán A.: J. Non. Cryst. Sol. *348*, 149 (2004).
16. Lakatos T., Johansson L.-G.: Glass. Tech. *13*, 88 (1972).
17. Fernandes R., Dilshat U.: Eur. Cer. Soc. *10*, 2283 (2012).
18. Adam J.G., Ellison C.: J. Non. Cryst. Sol. *127*, 247 (1991).
19. Greer J., Korkin A.: *Nano and Giga Challenges in Microelectronics*, p. 136, Elsevier Science, 2003.
20. Headley T.J., Loehman R.E.: J. Am. Cer. Soc.: *67*, 620 (1984).
21. El-Meliegy, E., van Noort, R.: *Glasses and glass ceramics for medical application*, Springer New York, 2012.
22. Fujimoto Y., Benino Y.: J. Cer. Soc. Jap. *109*, 466 (2001)
23. Karamanov A., Pelino M.: J. Eur. Cer. Soc. *19,* 649 (1999).
24. Kim K. D., Lee S. H.: J. Mat. Sci. *42,* 10180 (2007).
25. Moddeman W.E., Pence R.E., Massey R.T., Cassidy R.T. in: 3rd Annual Conference on Composites and Advanced Ceramic Materials, Part 2 of 2: Ceramic Engineering and Science Proceedings, p. 1394-1402, Ed. John B. Wachtman, The American Ceramic Society, Inc. 1989.